ELSEVIER

Contents lists available at ScienceDirect

Marine Pollution Bulletin

journal homepage: www.elsevier.com/locate/marpolbul



Three-layer trap: Congener-specific PCBs accumulation driven by the biological pump in the Sea of Japan

Min Yang ^a, Xinyu Guo ^{b,c,*}, Junyong Zheng ^{d,e}, Yasumasa Miyazawa ^c

- ^a State Key Laboratory of Satellite Ocean Environment Dynamics, Second Institute of Oceanography, Ministry of Natural Resources, 36 Baochu Road, Hangzhou, 310012. China
- ^b Center for Marine Environmental Studies, Ehime University, 2-5 Bunkyo-Cho, Matsuyama, 790-8577, Japan
- ^c Application Laboratory, Japan Agency for Marine-Earth Science and Technology, 3173-25, Showa-machi, Kanazawa-ku, Yokohama City, Kanagawa, 236-0001, Japan
- d State Key Laboratory of Physical Oceanography, Ocean University of China, 238 Songling Road, Qingdao, 266100, China
- e College of Oceanic and Atmospheric Sciences, Ocean University of China, 238 Songling Road, Qingdao, 266100, China

ARTICLE INFO

Keywords: Vertical stratification Accumulation factor Physicochemical property Semi-enclosed sea

ABSTRACT

A high-resolution, three-dimensional hydrodynamic–ecosystem–PCB model was applied to the Sea of Japan to investigate the roles of volatility and particle affinity in shaping the seasonal and spatial variations of four PCB congeners (CB28, CB101, CB153, and CB180). After a 21-year climatological simulation, their concentrations reveal a persistent three-layer vertical structure across all seasons, with dissolved PCBs maxima in the intermediate water (100–600 m). Although CB28 attains the highest absolute concentrations and CB180 the lowest, CB153 and CB101 exhibit the strongest subsurface enrichment, achieving summer accumulation factors of 2–6 compared with 1–4 for CB28 and CB180. Full-basin flux budgets reveal that relatively heavier congeners are more effectively scavenged onto particles during spring blooms and their subsequent sinking as well as remineralization sustain elevated intermediate layer dissolved pool. These findings demonstrate that, in strongly stratified, semi-enclosed basins with restricted exchange and long residence times, the oceanic biological pump preferentially sequesters high-chlorinated PCBs at intermediate water. This mechanism helps explain in situ observations of three-layer PCBs profiles and congener-specific depth trends. The modeling framework is readily transferable to other semi-enclosed seas and offers a predictive tool for assessing how intensified stratification under climate change may alter vertical pollutant fluxes and intermediate contaminant sinks.

1. Introduction

Persistent organic pollutants (POPs) particularly polychlorinated biphenyls (PCBs), are synthetic chemicals characterized by extreme toxicity and long-range transport potential (Berghuis and Roze, 2019; Lu et al., 2015; Xie et al., 2019). Despite the production ban in the late 1970s, PCBs remain ubiquitous in the global ocean due to their hydrophobicity and strong affinity for organic matter, allowing them to accumulate and biomagnify within food webs (Breivik et al., 2007; Joyce et al., 2016; Ma et al., 2018; Sobek et al., 2023). Even trace levels of dissolved PCBs in seawater correspond to significant burdens in plankton and higher trophic levels, sustaining ecological and human health risks long after emissions ceased (Bargagli and Rota, 2024; Dachs et al., 2002; Froescheis et al., 2000; Gustafsson and Andersson, 2012; Jamieson et al., 2017; Sobek et al., 2004).

Deep-sea ecosystems, once considered remote and pristine, now register measurable PCBs burdens delivered by atmospheric deposition, ocean currents, and anthropogenic activities (Sanganyado et al., 2021). Vertical structures of PCBs in the open ocean often show "nutrient-like" patterns, with low concentrations at the surface and enrichment in intermediate and deep waters (Sobek and Gustafsson, 2014; Sun et al., 2016). Field studies have documented dissolved PCBs concentrations several-fold higher in deep layers than at the surface in the Arctic, Atlantic, and Indian Oceans (Booij et al., 2014; Lohmann et al., 2006; Schulz-Bull et al., 1998). Importantly, different congeners exhibit contrasting degrees of deep accumulation. For instance, Schulz-Bull et al. (1998) reported that hexa- and hepta-chlorinated congeners (e.g., CB153, CB180) were disproportionately enriched in intermediate and deep waters of the North Atlantic compared with lighter congeners such as CB28. These observations suggest active vertical transport and long-

^{*} Corresponding author at: Center for Marine Environmental Studies, Ehime University, 2-5 Bunkyo-Cho, Matsuyama, 790-8577, Japan. *E-mail address*: guo.xinyu.mz@ehime-u.ac.jp (X. Guo).

term sequestration of heavier congeners in open-ocean. However, whether similar or even enhanced accumulation patterns occur in semi-enclosed basins remains uncertain. Due to restricted lateral exchange and strong seasonal stratification, such basins may amplify vertical trapping, potentially intensifying the buildup of POPs like PCBs.

Numerical fate models are indispensable for elucidating PCBs vertical distributions. At the global scale, models that incorporate congener-specific air–sea exchange and ocean circulation successfully reproduce broad latitudinal PCBs trends (Lammel and Stemmler, 2012) and, more recently, simulate the three-dimensional behavior of multiple congeners under climate-driven changes in biogeochemistry (Wagner et al., 2019). However, these global approaches lack the spatial resolution and process detail, particularly bloom-driven particle fluxes and deep-water exchanges, which are required to capture the seasonally stratified dynamics of the semi-enclosed seas. Regionally, coupled hydrodynamic–ecosystem–PCB model have quantified PCBs fate and transportation in the northwestern Pacific and its marginal seas (Yang et al., 2024; Yang et al., 2022).

The Sea of Japan (SoJ) is a representative marginal sea of the northwestern Pacific with bowl-shaped bathymetry and limited water exchange through shallow straits (<150 m), resulting in prolonged residence times and pronounced seasonal stratification (Isobe, 2020; Oba and Irino, 2012). These features make it particularly susceptible to subsurface contaminant trapping. Kannan et al. (1998) observed maxima of more than 30 congeners in the SoJ between 100 and 500 m, with CB101 and CB153 showing much stronger subsurface peaks than lighter congeners. A recent coupled hydrodynamic-ecosystem-PCB model revealed that CB153 forms a three-layer vertical structure in the SoJ, with intermediate-water maxima sustained by particle export and remineralization (Yang et al., 2024). However, that study focused solely

on CB153, leaving open the question of whether other congeners, differing in volatility and particle affinity, follow the same accumulation patterns.

Here, we extend the modeling framework (Yang et al., 2024) to four representative congeners (CB28, 101, 153, and 180), spanning a wide range of physicochemical properties. By integrating congener-specific air-sea exchange, particle uptake, remineralization, and strait exchanges into a basin-wide flux budget, we quantify how these processes jointly establish steady-state vertical structure. In doing so, we highlight the difference in the accumulation potential among congeners in deep water. Beyond the SoJ, our findings offer a transferable framework for understanding pollutant cycling in other semi-enclosed basins, with broader implications for ecosystem exposure.

2. Materials and methods

The SoJ is a semi-enclosed marginal basin of the northwestern Pacific, with a characteristic bowl-shaped bathymetry reaching nearly 3800 m at its deepest point (Fig. 1). Its connections to the open Pacific lie through four relatively shallow straits, each no more than 150 m. Because these sills restrict water exchange to the upper 200 m, the intermediate and deep-water masses of the SoJ remain largely isolated, allowing unique physical and biogeochemical conditions to develop in its interior (Isobe, 2020; Isobe, 2008; Lee et al., 2008; Yanagi, 2002). In addition, enhanced spring–summer phytoplankton blooms in the northern SoJ may scavenge dissolved PCBs more efficiently (Takahashi et al., 2014).

We extended the three-dimensional hydrodynamic-ecosystem-PCB coupled framework described in Yang et al. (2024) to examine congener-specific accumulation in the SoJ. The ocean circulation fields

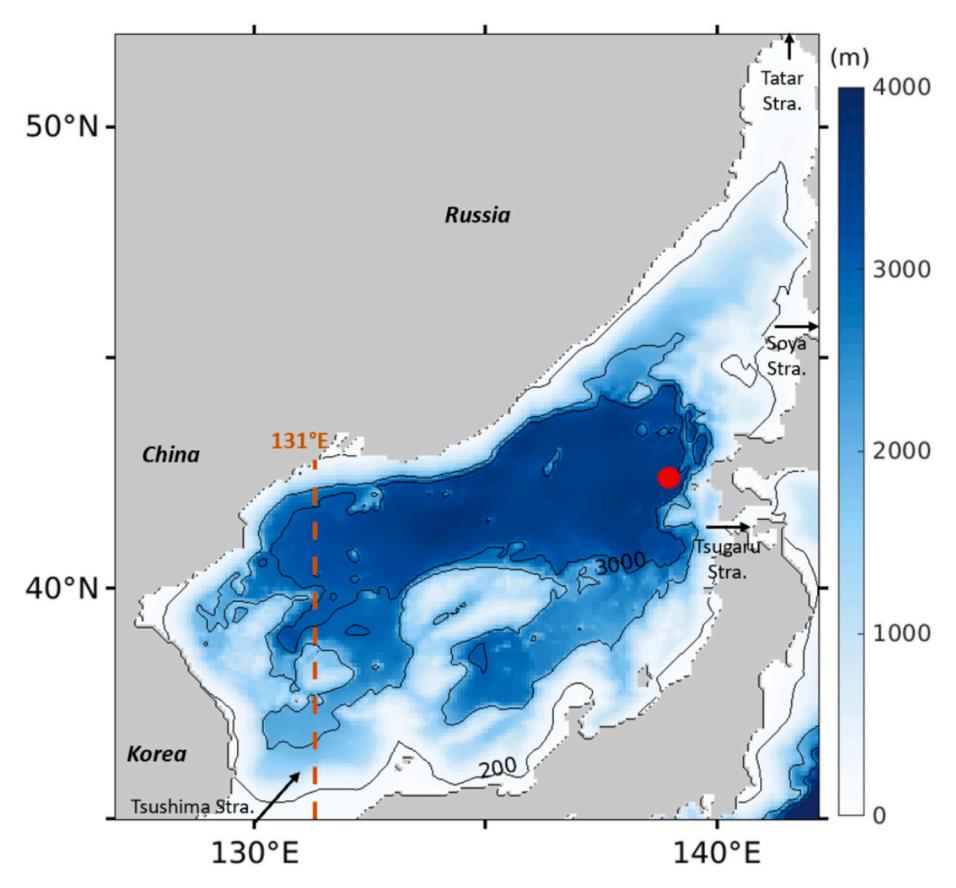


Fig. 1. Bathymetric map of model domain of the Sea of Japan (SoJ). Orange dashed line denotes the 131°E section. Red filled circle denotes the position of the Siribesi Trough. Black arrows represent surface currents in the straits as demonstrated by the previous study (Talley et al., 2004). (For interpretation of the references to colour in this figure legend, the reader is referred to the web version of this article.)

are supplied by JCOPE2M (Japan Coastal Ocean Predictability Experiment 2, http://www.jamstec.go.jp/jcope/), which is built on the Princeton Ocean Model and configured at 1/12° horizontal resolution with 47 vertical levels (Miyazawa et al., 2017; Miyazawa et al., 2009). JCOPE2M provides daily three-dimensional fields of temperature, salinity, horizontal and vertical velocity components, and eddy diffusivity coefficients. More details are given in Supporting Information (Text S1) The ecosystem module simulates key pelagic components (nitrate, phytoplankton, zooplankton, and detritus) and their exchanges (growth, mortality, sinking and remineralization). And this module provides daily biomass, mortality rate of phytoplankton, and the decomposition rate and sinking velocity of detritus. Full ecosystem equations and parameter values follow the previous work (Ishizu et al., 2021) and are summarized in Supporting Information (Text S2). These two fields are used offline to drive the PCBs transport modules. The PCB module explicitly tracks dissolved and particulate phases of each congener subject to oceanic advection and diffusion, air-sea exchange, biological uptake onto phytoplankton and detritus, sinking of particulate PCBs with detritus, remineralization of particle-bound PCBs back to the dissolved pool, and photolytic degradation of the dissolved phase. All model formulations for mass exchange and degradation follow Yang et al. (2022, 2024) and Text S3-S4 in Supporting Information.

In contrast to earlier work that focused exclusively on a single congener (CB153), our study simultaneously examines four PCB congeners of CB28, 101, 153, and 180, each spanning a distinct range of molecular weight, volatility, and particle-water partitioning behavior. Table S1 lists the numerical values and literature sources for all PCB-specific parameters used in this study. Photolytic degradation of dissolved PCBs is parameterized as depth-dependent approach (Yang et al., 2024). By incorporating congener-specific H' and particle-affinity parameters (Del Vento and Dachs, 2002; Li et al., 2003; Sinkkonen and Paasivirta, 2000), we ensure that each compound's unique physicochemical fingerprint is represented in model physics and biogeochemistry. This multi-congener approach allows us to answer how differences in volatility and sorption translate into divergent accumulation patterns in the semi-enclosed environment of the SoJ.

We address these questions by conducting a 21-year of simulation

under repeated climatological forcing and initializing all four congeners at zero and allowing the model to evolve until it reaches a quasi-steady annual cycle. We treat the first 20 years of simulations as spin-up period and perform our analysis for each physical and biogeochemical process using model results in the 21st simulation year. We calculate full-domain, monthly integrals of all major source and sink processes. Drawing from the previous framework (Yang et al., 2024), which demonstrated the three-layer accumulation of CB153, these novel extensions reveal congener-specific controls on intermediate water PCBs accumulation.

3. Results and discussion

3.1. Spatial and temporal variations of four congeners

Dissolved concentrations of the four PCB congeners in the SoJ exhibit both clear seasonal cycles and north-south gradients (Fig. 2). Across all seasons, CB28 reaches the highest surface concentrations (\sim 1.0–2.5 pg L^{-1}), followed by CB101 (0.5–1.5 pg L^{-1}), CB153 (0.2–1.0 pg L^{-1}), and CB180 (0.1–0.5 pgL^{-1}). These magnitude differences reflect the relative atmospheric loadings that the atmospheric concentration of CB28 is roughly 4, 8, and 20 times larger than that of CB101, 153, and 180, respectively (Fig. S5). The concentrations of all congeners peak in summer and reach minima in autumn. In summer, surface concentrations are consistently higher in the southern SoJ than in the northern SoJ, driven by intensified atmospheric deposition and advection of PCBs-rich Tsushima Warm Current waters (Yang et al., 2022). By contrast, in autumn through spring, the gradient inverts. Cooler northern surface waters enhance downward air-sea exchange, elevating the northern dissolved concentrations above those in the south (Lammel and Stemmler, 2012).

Particulate PCBs display a broadly consistent spatiotemporal pattern. Their concentrations are greatest in the northern basin, peak in spring (Fig. 3b), and then decline through summer into winter. This spring maximum coincides with the spring bloom of phytoplankton in the northern SoJ (Fig. S3), whose abundant biomass scavenges dissolved PCBs and transfers them into the particulate pool (Booij et al., 2014;

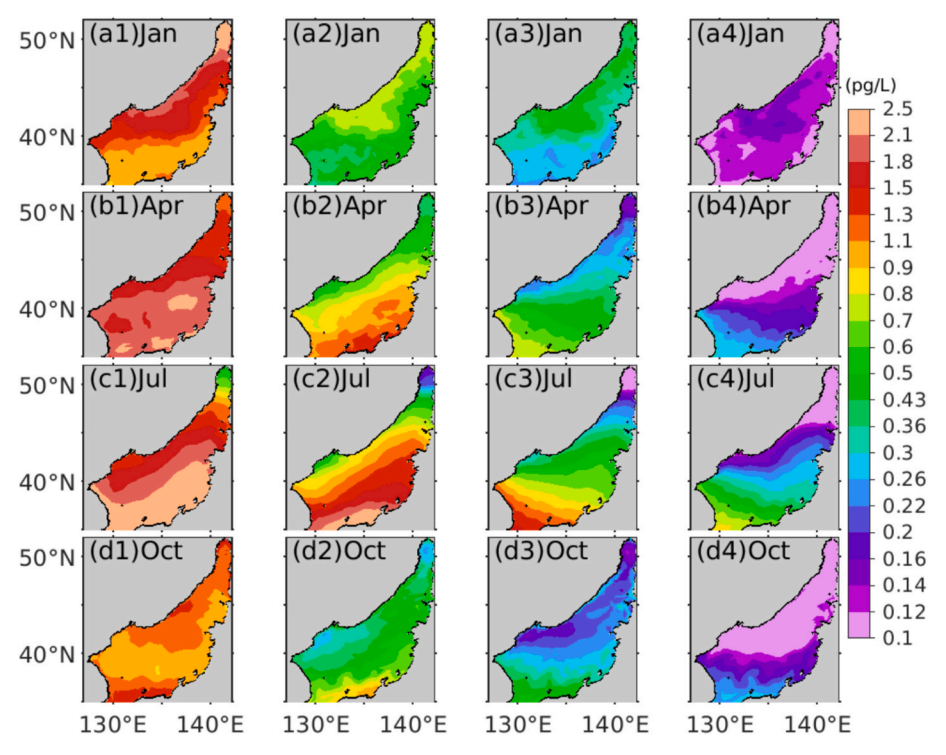


Fig. 2. Horizontal distributions of surface dissolved (a1-d1) CB28, (a2-d2) CB101, (a3-d3) CB153, and (a4-d4) CB180 concentrations.

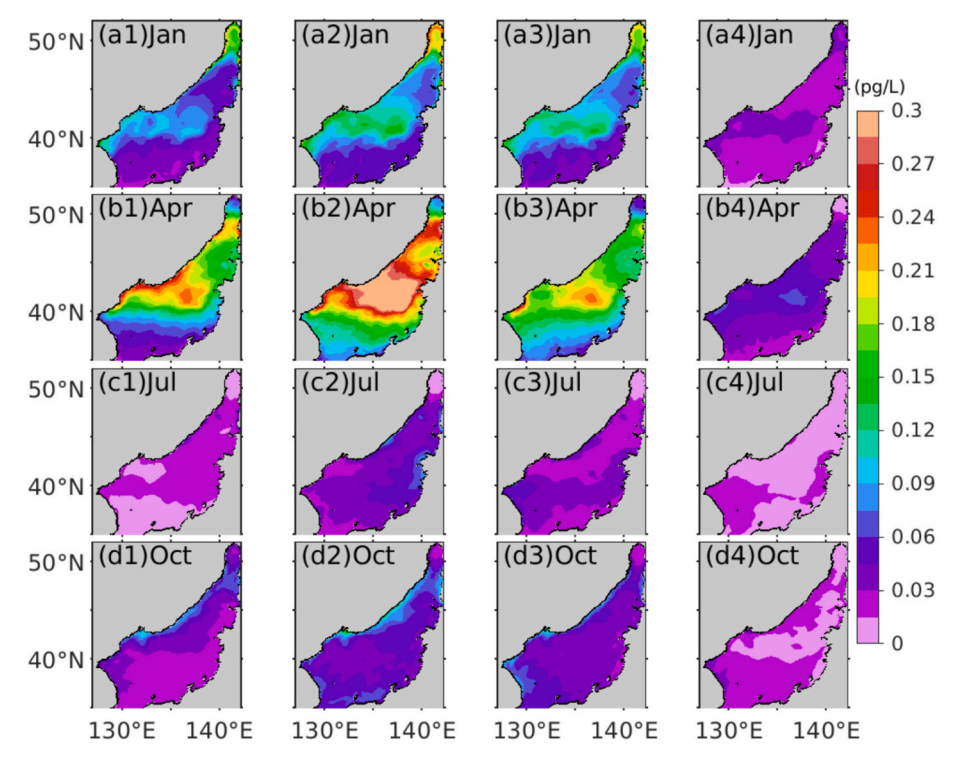


Fig. 3. Horizontal distributions of surface particle-bound (a1-d1) CB28, (a2-d2) CB101, (a3-d3) CB153, and (a4-d4) CB180 concentrations.

Lohmann et al., 2006; Yang et al., 2024). However, the relative ordering of congeners in the particulate phase departs markedly from both their dissolved-phase magnitudes and their nominal hydrophobicity. CB101 exhibits the highest particle-bound concentrations (Fig. 3 b2), although CB28 possesses the largest dissolved concentrations and CB153/CB180 have stronger bioconcentration factors (BCF) (Table S1). This mismatch indicates that simple partitioning alone cannot explain particle association; rather, congener-specific differences in phytoplankton and

detritus uptake kinetics, and subsequent remineralization must also be responsible for the observed particulate PCBs distributions.

We chose the 131°E section (orange dashed line in Fig. 1) to illustrate PCBs vertical structure because it intersects both the Tsushima Warm Current in the south and the Liman Cold Current in the north, captures the most pronounced three-layer PCBs structure. Along this transect, all four congeners develop the characteristic of three-layer accumulation, with a pronounced concentration maximum in the intermediate layer

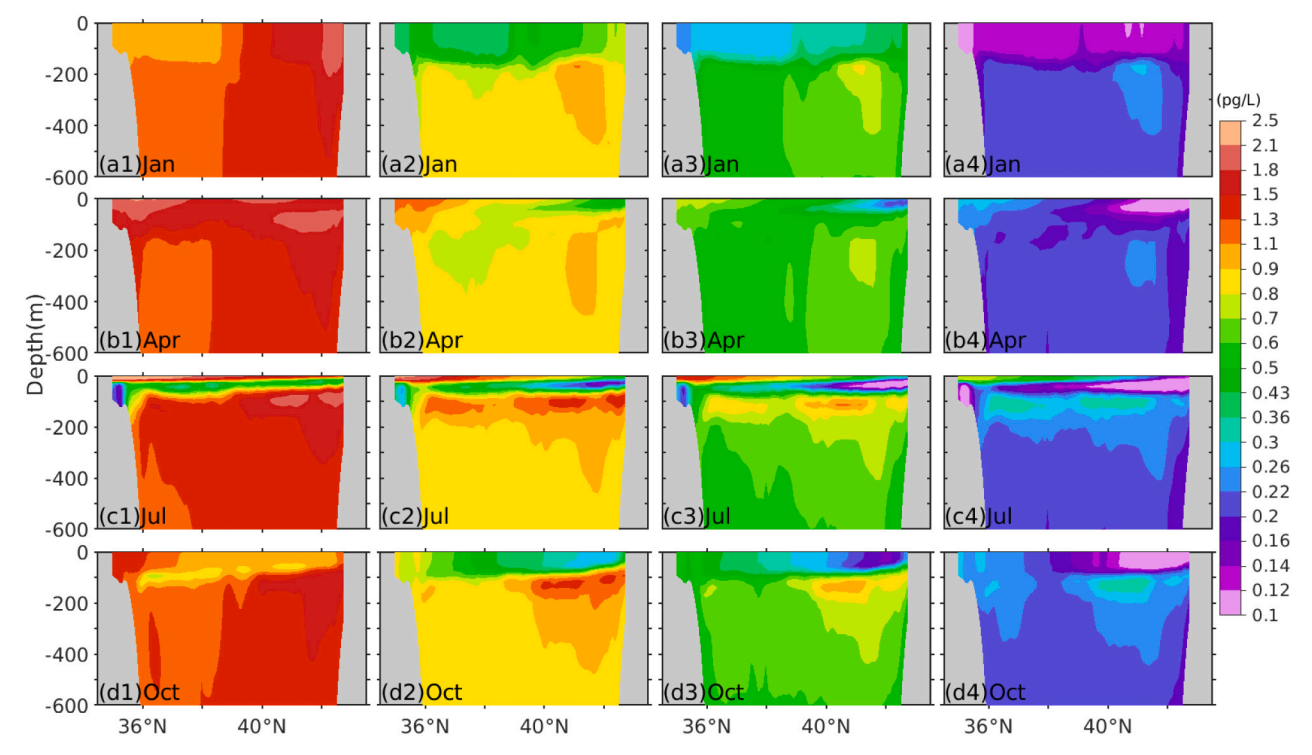


Fig. 4. Vertical distributions of dissolved (a1-d1) CB28, (a2-d2) CB101, (a3-d3) CB153, and (a4-d4) CB180 (a1-a4) concentrations along section 131°E.

(100–600 m) and systematically higher values in the northern basin compared to the south (Fig. 4). Notably, however, CB28 deviates from the other congeners by lacking a subsurface maximum beneath the mixed layer in winter, its dissolved concentration below 100 m remains essentially comparable to that within the surface mixed layer (Fig. 4 a1). By contrast, CB101, 153, and 180 all sustain elevated concentrations at depths greater than 100 m, reflecting their stronger retention in the intermediate water.

Although deep-water PCBs observations in the SoJ are scant, the Siribesi Trough (red filled circle in Fig. 1) profiles reported dissolved maxima for over 30 congeners between 100 and 500 m (Kannan et al., 1998). These data, despite omitting CB28, rank CB101 highest in the intermediate water, followed by CB153 and then CB180, in exact agreement with their rankings in our model results. This correspondence between in situ measurements and simulation underlines the reliability of our three-layer accumulation pattern throughout the SoJ.

Seasonally, the vigorous convective mixing in winter homogenizes the upper water column, flushes PCBs downward and produces an almost uniform concentration down to the bottom of surface mixed layer (Fig. 4 a1-a4). As the stratification develops and the surface mixed layer becomes shallow from spring to summer, these winter stored PCBs become trapped just below the shallow mixed layer, forming a conspicuously high concentration patch around 100 m (Fig. 4c). When the next winter overturn occurs, this subsurface maximum is reentrained into the surface mixed layer and diluted by the relatively uncontaminated surface waters. In the absence of biochemical sources, physical mixing alone would drive intermediate layer concentrations asymptotically toward but never above the surface level over the repeated seasonal cycles.

Our results reveal that, in summer and autumn, the intermediate layer concentrations of these congeners actually surpass those at the surface, indicating an additional interior source of dissolved PCBs during stratified months. Examination of particulate-phase profiles (Fig. 5b) shows a springtime peak in particle-bound PCBs within the upper 100 m, followed by a decline through summer, indicative of ongoing detritus remineralization. As phytoplankton and detritus laden with PCBs continue sinking unabated across the thermocline, their decomposition in the subsurface releases a pulse of dissolved PCBs that fuels and sustains the summer subsurface maximum (Fig. 5c). Differences in the magnitude of this enrichment among congeners reflect their physicochemical traits that congeners with higher BCF experience stronger scavenging onto particles and thus more efficient delivery to depth, while those with higher volatility undergo greater air–sea exchange losses, modulating the net strength of the biological pump.

To quantify the subsurface enrichment among congeners, we introduce an accumulation factor (AF), defined as the ratio of dissolved concentration between the upper 600 m and that in the surface layer. Along the 131°E section, AF is uniformly larger than 1 below 100 m, particularly in the northern basins (Fig. 6). CB28 exhibits a low AF (1–2), reflecting its strong surface inputs and limited particle removal. In contrast, CB101 and CB153 reach AFs of 2-5 and 3-6, respectively, while CB180 falls in between (3-4). Seasonal modulation of AF is dramatic. In winter, AFs below 100 m depth barely exceeds 2 (Fig. 6 a1-a4), reflecting homogenizing convective mixing and elevated surface concentrations from enhanced air-sea exchange. By summer, the pronounced stratification isolates the surface layer and AFs at 100 m rises modestly (about 1.5-3.0 depending on congeners). In autumn, despite similar intermediate layer dissolved concentrations, surface concentration falls sharply causing AFs to peak (2–6) (Fig. 6 d1-d4). This seasonal progression underscores the dual control of AFs by biogeochemical supply at depth and by surface concentration declines.

In addition, field observations in the Siribesi Trough report midwater AFs of >10 for CB153, 6–8 for CB101, and < 5 for both light (e. g. CB52) and very heavy (CB180) congeners (Kannan et al., 1998), which precisely mirroring our modeled hierarchy. This strong agreement validates our coupled physical–biogeochemical framework. For this reason, we expect that the same three-layer accumulation mechanisms also operate in other semi-enclosed basins.

3.2. Budget of PCB fluxes driving congener-specific accumulation

To elucidate the key processes shaping PCBs spatiotemporal distributions and the AFs, we completed a full budget analysis of dissolved PCB fluxes across the entire SoJ (Fig. 7). In winter and early spring, the air-sea exchange delivers the bulk of dissolved CB28 and CB101, whereas CB153 and CB180 receive much smaller direct inputs. As the spring bloom matures, combined uptake by phytoplankton and detritus removes on the magnitudes of 2, 7, 4, and 2 $kg d^{-1}$ of CB28, 101, 153, and 180, respectively. However, the downward air-sea exchange flux of CB28 is so large relative to its particle uptake that only a tiny fraction of CB28 ever becomes particle-bound. Furthermore, much of the PCBs that does adsorb onto particles are quickly liberated again by remineralization, so that net particulate stocks remain low for all congeners. During summer, PCBs experience a sharp decline in net atmospheric input as warmer surface waters enhance volatilization. By autumn, the direction of air-sea exchange for CB101, CB153, and CB180 even reverses, leading to a net loss to the atmosphere. Notably, the net flux of CB28 is negative around the year due to the large self-degradation flux, indicating that its

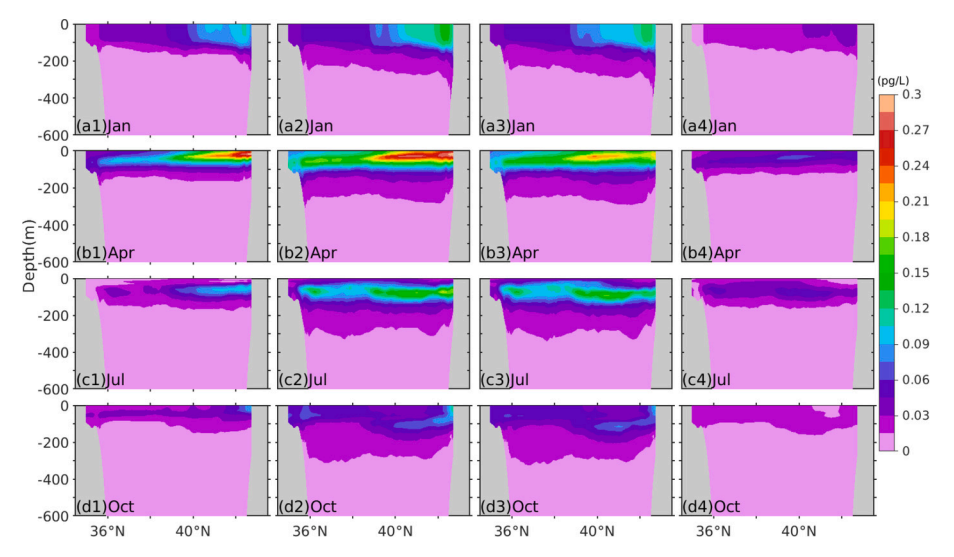


Fig. 5. Vertical distributions of particle-bound (a1-d1) CB28, (a2-d2) CB101, (a3-d3) CB153, and (a4-d4) CB180 concentrations along section 131°E.

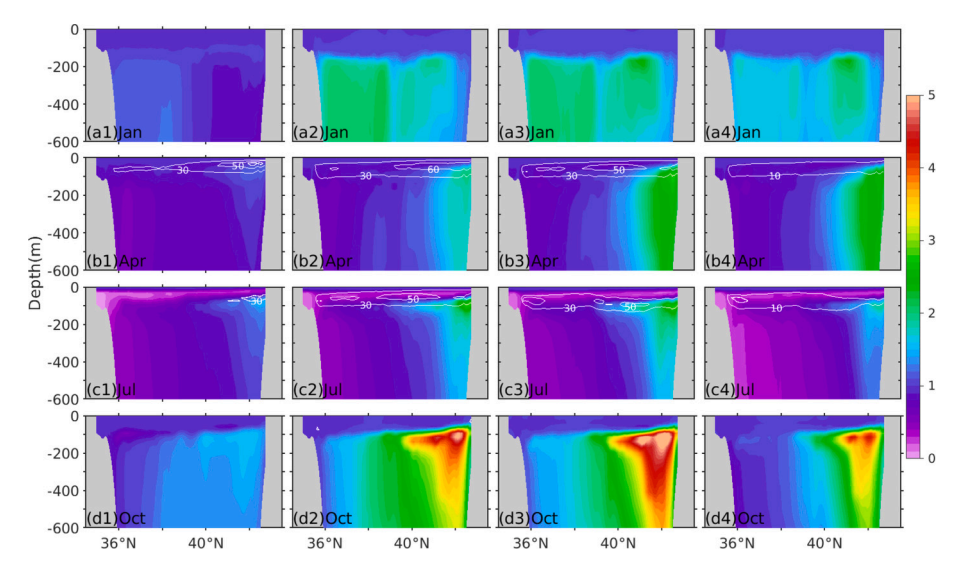


Fig. 6. Vertical distributions of the AF for (a1–d1) CB28, (a2–d2) CB101, (a3–d3) CB153, and (a4–d4) CB180 along section 131° E (unitless). White solid lines represent the remineralization flux of the dissolved PCBs ($ug d^{-1}$) for each grid point.

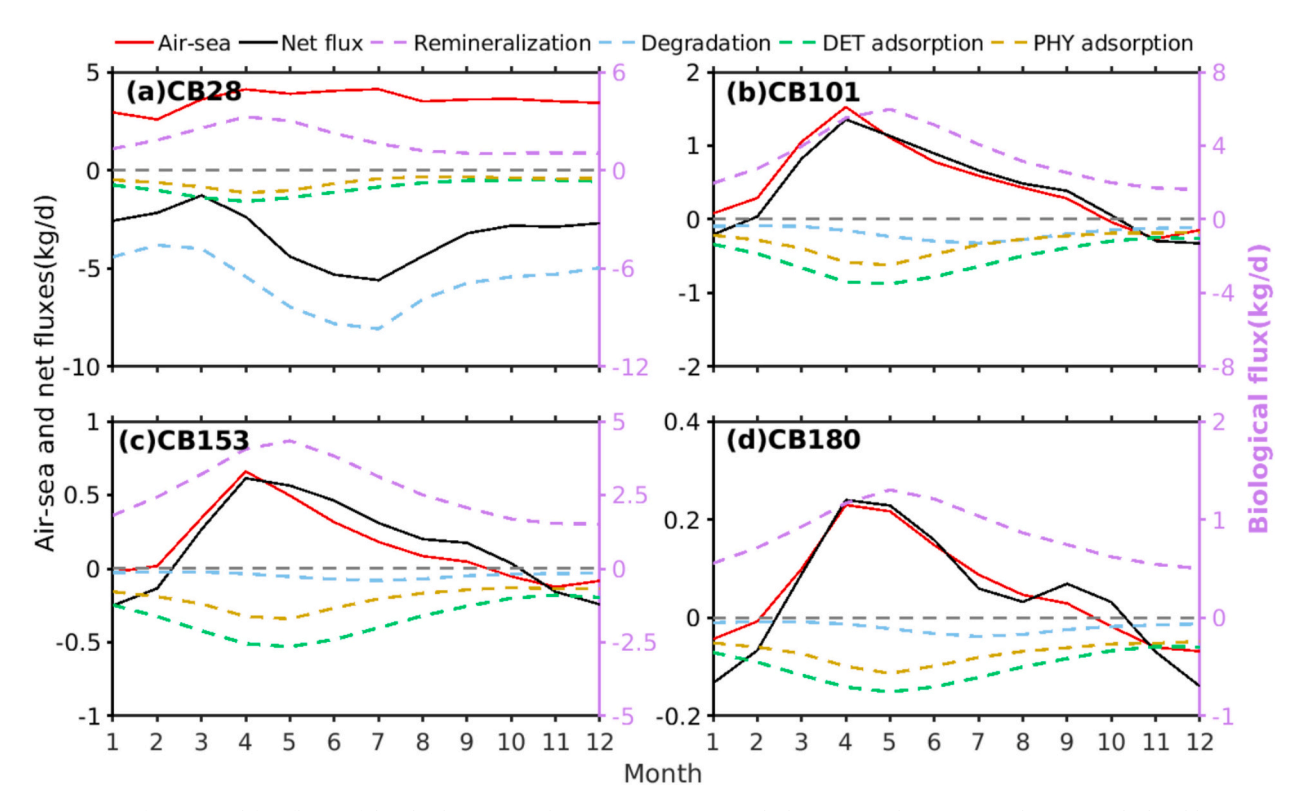


Fig. 7. Time series of source and fate fluxes of dissolved (a) CB28, (b) CB101, (c) CB153, and (d) CB180 in the seawater. Fluxes are calculated by integrating the whole space of the SoJ. The air–sea exchange flux is represented by the red solid line, with a scale shown on left axis. The biological fluxes are represented by the dashed lines including phytoplankton adsorption (brown), detritus adsorption (green), and detritus remineralization (purple), with a scale shown on the right axis. The net flux of dissolved PCBs is represented by the solid black line, with a scale shown on the left axis. The self-degradation flux of dissolved PCBs is represented by the dashed cyan line, with a scale shown on the right axis. Positive fluxes are defined to increase the dissolved PCBs concentration in the seawater. "PHY" denotes phytoplankton; "DET" denotes detritus. (For interpretation of the references to colour in this figure legend, the reader is referred to the web version of this article.)

short half-life expressed by degradation in Fig. 7 results in CB28 being unable to remain in water for a long time. Reversely, the other three congeners show much smaller degradation flux and positive net flux, suggesting prominent accumulation. The PCBs transport fluxes through the lateral straits were minimal compared with the air-sea input and biological fluxes (Fig. 7); therefore, they were not included in the comparison for the fluxes.

Differing from dissolved PCBs, the seasonal and spatial patterns of

particulate PCBs are governed almost entirely by the dynamic balance between congener-specific scavenging and remineralization (Fig. 8). During winter and spring, all four congeners exhibit their highest net transfer fluxes into the particulate phase, affected by cold water temperature and elevated phytoplankton biomass. In summer, the net conversion of dissolved PCBs to particles falls to its annual minimum; concurrently, the spring–summer peak in particulate remineralization flux indicates extensive dissolution of particle-bound PCBs back into the

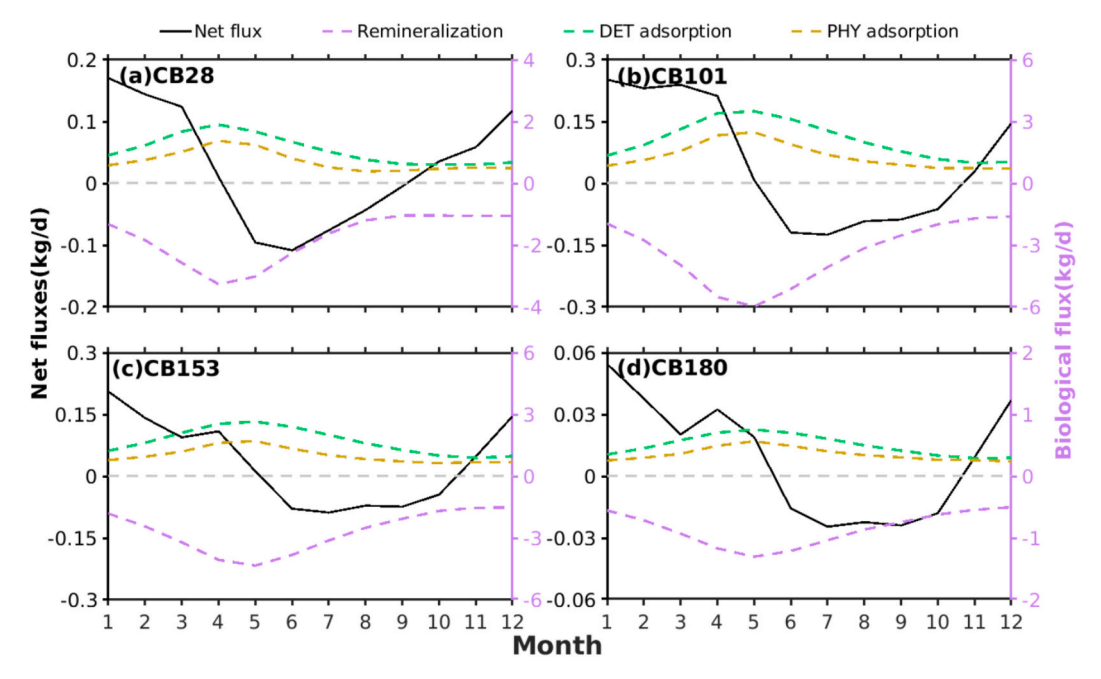


Fig. 8. The same as Fig. 7 but for particulate (a) CB28, (b) CB101, (c) CB153, and (d) CB180 in the seawater.

water column. Among congeners, CB101 shows the strongest springtime net particulate uptake (Fig. 8b), whereas CB180 remains the least efficiently scavenged into particles (Fig. 8d). The particulate PCBs transport fluxes through the lateral straits were minimal compared with the biological fluxes (Fig. 8); therefore, they were not included in the comparison for the fluxes.

Congener-specific AFs ranges reflect the physicochemical behavior of PCB congeners. Despite its large atmospheric deposition, CB28 shows the smallest AF, since its low BCF limits subsurface delivery and sustained air-sea exchange maintains a high surface reservoir. All congeners peak in particles remineralization between 60 and 100 m during spring-summer (white solid line in Fig. 6). However, despite its exceptionally high remineralization flux delivering the largest subsurface supply, the autumn deepening of the mixed layer re-entrains much of CB101 into the surface layer, leading to substantial volatilization losses (Fig. 7b). In contrast, though CB153 supplied more modestly by remineralization, it undergoes minimal autumnal loss to the atmosphere (Fig. 7c), allowing a greater net retention of mass below the thermocline. CB180, with the weakest uptake and remineralization, achieves only intermediate enrichment.

To isolate the influence of congener physicochemical properties, we then treated all four congeners as if they shared identical atmospheric input fluxes. The resulting accumulation factors (AFs) reveal that CB153 and CB101 concentrate in the intermediate layer at rates several-fold higher than CB28, even under equal surface loading. This divergence highlights how small differences in volatility and particle affinity are dramatically amplified by the biological pump and subsurface remineralization, ultimately dictating congener-specific deep-water accumulation.

In a sense, our investigation of deep-water accumulation for these four congeners serves as a sensitivity test of their physicochemical properties. Were all four supplied with identical atmospheric inputs, the calculated AFs indicate that CB153 and CB101 would build up in the intermediate layer far more strongly than CB28. This divergence underscores how small differences in volatility and particle affinity can be dramatically amplified by the biological pump and subsurface remineralization, ultimately dictating congener-specific deep-water accumulation.

4. Conclusion

This study demonstrates that the differential accumulation potential of PCB congeners in the intermediate waters of the SoJ arises from the interplay of congener-specific air-sea exchange, bio-particles sorption, and remineralization fluxes under a strongly stratified, semi-enclosed basin. Springtime scavenging by phytoplankton and detritus loads particles with PCBs near the surface, as well as the continuously sinking of these particles through the thermocline and undergo remineralization below the shallow mixed layer in summer are all responsible for the accumulation of PCB in the intermediate waters. The resulting remineralization flux injects PCBs into the subsurface dissolved pool, creates an intermediate layer concentration maximum that exceeds what winter mixing alone would produce. By depicting the seasonal and spatial patterns for CB28, 101, 153, and 180, along with quantifying their accumulation factors and biogeochemical flux budgets, we demonstrate CB153 as the most prone to intermediate layer enrichment and CB28 the least, despite its large atmospheric input. These results not only elucidate mechanistic controls on deep-sea contaminant sinks in a semienclosed sea but also provide a rigorous framework for interpreting congener-dependent pollutant dynamics in any similarly isolated basin.

Our findings have three broad implications. First, the pronounced subsurface maxima of dissolved PCBs indicate an elevated exposure potential for mid-water and benthopelagic biota. Because our model does not simulate bioaccumulation or trophic transfer, we recommend targeted subsurface monitoring and future coupling with bioaccumulation models to quantify species-level risk. Second, as climate warming intensifies summer stratification, two opposing effects on PCBs accumulation can be predicted. On one hand, a shallower mixed layer will weaken the winter mixing leaving more PCBs locked below the thermocline, boosting intermediate-water enrichment over successive years. On the other hand, stronger stratification can suppress nutrient upwelling, reduce phytoplankton production and particle export, weaken the biological pump, and thereby decrease subsurface delivery of PCBs. Finally, by distilling these processes into a semi-enclosed basin paradigm, where there is restricted water exchange with outside, seasonal bloom-driven particle export, and congener-specific remineralization converge, this work offers a transferable model for knowing pollutant cycling in other enclosed seas and fjords. For example, the Norway's Sognefjord and the Baltic Sea, which shares strong stratification and limited exchange, are ideal candidates for applying this semi-enclosed basin framework.

CRediT authorship contribution statement

Min Yang: Writing – review & editing, Writing – original draft, Validation, Methodology, Formal analysis, Data curation, Conceptualization. Xinyu Guo: Writing – review & editing, Supervision, Methodology, Formal analysis, Conceptualization. Junyong Zheng: Writing – review & editing. Yasumasa Miyazawa: Writing – review & editing.

Declaration of competing interest

The authors declare that they have no known competing financial interests or personal relationships that could have appeared to influence the work reported in this paper.

Acknowledgments

The authors declare no conflicts of interest relevant to this study. We are grateful to Carey L. Friedman and Noelle Eckley Selin for providing the atmospheric PCBs data. M.Y was supported by the Scientific Research Fund of the Second Institute of Oceanography, MNR (grant no. JB2503). X. G was supported by the Moonshot Research and Development Program (Grant no. JPNP18016), and the New Energy and Industrial Technology Development Organization (NEDO). The authors also thank support from the Ministry of Education, Culture, Sports, Science and Technology, Japan (MEXT) for a project on Joint Usage/Research Center—Leading Academia in Marine and Environment Pollution Research (LaMer).

Appendix A. Supplementary data

Supplementary data to this article can be found online at https://doi.org/10.1016/j.marpolbul.2025.118796.

Data availability

Data will be made available on request.

References

- Bargagli, R., Rota, E., 2024. Environmental contamination and climate change in Antarctic ecosystems: an updated overview. Environ. Sci.: Adv. 3, 543–560. https://doi.org/10.1039/D3VA00113J.
- Berghuis, S.A., Roze, E., 2019. Prenatal exposure to PCBs and neurological and sexual/pubertal development from birth to adolescence. Curr. Probl. Pediatr. Adolesc. Health Care 49, 133–159. https://doi.org/10.1016/j.cppeds.2019.04.006.
- Booij, K., van Bommel, R., van Aken, H.M., van Haren, H., Brummer, G.-J.A., Ridderinkhof, H., 2014. Passive sampling of nonpolar contaminants at three deepocean sites. Environ. Pollut. 195, 101–108. https://doi.org/10.1016/j. envpol.2014.08.013.
- Breivik, K., Sweetman, A., Pacyna, J.M., Jones, K.C., 2007. Towards a global historical emission inventory for selected PCB congeners — a mass balance approach: 3. An update. Sci. Total Environ. 377, 296–307. https://doi.org/10.1016/j. scitotenv.2007.02.026.
- Dachs, J., Lohmann, R., Ockenden, W.A., Méjanelle, L., Eisenreich, S.J., Jones, K.C., 2002. Oceanic biogeochemical controls on global dynamics of persistent organic pollutants. Environ. Sci. Technol. 36, 4229–4237. https://doi.org/10.1021/ es0/57/24k
- Del Vento, S., Dachs, J., 2002. Prediction of uptake dynamics of persistent organic pollutants by bacteria and phytoplankton. Environ. Toxicol. Chem. 21, 2099–2107. https://doi.org/10.1002/etc.5620211013.
- Froescheis, O., Looser, R., Cailliet, G.M., Jarman, W.M., Ballschmiter, K., 2000. The deep-sea as a final global sink of semivolatile persistent organic pollutants? Part I: PCBs in surface and deep-sea dwelling fish of the North and South Atlantic and the Monterey Bay Canyon (California). Chemosphere 40, 651–660. https://doi.org/10.1016/S0045-6535(99)00461-0.
- Gustafsson, Ö., Andersson, P.S., 2012. 234Th-derived surface export fluxes of POC from the Northern Barents Sea and the Eurasian sector of the Central Arctic Ocean. Deep-Sea Res. I Oceanogr. Res. Pap. 68, 1–11. https://doi.org/10.1016/j.dsr.2012.05.014.

- Ishizu, M., Miyazawa, Y., Guo, X., 2021. Long-term variations in ocean acidification indices in the Northwest Pacific from 1993 to 2018. Clim. Chang. 168, 29. https://doi.org/10.1007/s10584-021-03239-1.
- Isobe, A., 2008. Recent advances in ocean-circulation research on the Yellow Sea and East China Sea shelves. J. Oceanogr. 64, 569–584. https://doi.org/10.1007/s10872-008-0048-7.
- Isobe, A., 2020. Paleo-ocean destratification triggered by the subduction of the Oyashio water into the Sea of Japan after the last glacial maximum. Paleoceanogr. Paleoclimatol. 35, e2019PA003593. https://doi.org/10.1029/2019PA003593.
- Jamieson, A.J., Malkocs, T., Piertney, S.B., Fujii, T., Zhang, Z., 2017. Bioaccumulation of persistent organic pollutants in the deepest ocean fauna. Nat. Ecol. Evol. 1, 1–4. https://doi.org/10.1038/s41559-016-0051.
- Joyce, A.S., Portis, L.M., Parks, A.N., Burgess, R.M., 2016. Evaluating the relationship between equilibrium passive sampler uptake and aquatic organism bioaccumulation. Environ. Sci. Technol. 50, 11437–11451. https://doi.org/10.1021/acs.est.6b03273.
- Kannan, N., Yamashita, N., Petrick, G., Duinker, J.C., 1998. Polychlorinated biphenyls and nonylphenols in the Sea of Japan. Environ. Sci. Technol. 32, 1747–1753. https://doi.org/10.1021/es970713q.
- Lammel, G., Stemmler, I., 2012. Fractionation and current time trends of PCB congeners: evolvement of distributions 1950–2010 studied using a global atmosphere-ocean general circulation model. Atmos. Chem. Phys. 12, 7199–7213. https://doi.org/ 10.5194/acp-12-7199-2012.
- Lee, T., Hyun, J.-H., Mok, J.S., Kim, D., 2008. Organic carbon accumulation and sulfate reduction rates in slope and basin sediments of the Ulleung Basin, East/Japan Sea. Geo-Mar. Lett. 28, 153–159. https://doi.org/10.1007/s00367-007-0097-8.
- Li, N., Wania, F., Lei, Y.D., Daly, G.L., 2003. A comprehensive and critical compilation, evaluation, and selection of physical–chemical property data for selected polychlorinated biphenyls. J. Phys. Chem. Ref. Data Monogr. 32, 1545–1590. https://doi.org/10.1063/1.1562632.
- Lohmann, R., Jurado, E., Pilson, M.E.Q., Dachs, J., 2006. Oceanic deep water formation as a sink of persistent organic pollutants. Geophys. Res. Lett. 33. https://doi.org/ 10.1029/2006GL025953.
- Lu, D., Lin, Y., Feng, C., Wang, D., She, J., Shen, H., Wang, G., Zhou, Z., 2015. Levels of polychlorinated dibenzo-p-dioxins/furans (PCDD/Fs) and dioxin-like polychlorinated biphenyls (DL-PCBs) in breast milk in Shanghai, China: a temporal upward trend. Chemosphere 137, 14–24. https://doi.org/10.1016/j. chemosphere.2015.04.043.
- Ma, Y., Adelman, D.A., Bauerfeind, E., Cabrerizo, A., McDonough, C.A., Muir, D., Soltwedel, T., Sun, C., Wagner, C.C., Sunderland, E.M., Lohmann, R., 2018. Concentrations and water mass transport of legacy POPs in the Arctic Ocean. Geophys. Res. Lett. 45, 12,972–12,981. https://doi.org/10.1029/2018GL078759.
- Miyazawa, Y., Zhang, R., Guo, X., Tamura, H., Ambe, D., Lee, J.-S., Okuno, A., Yoshinari, H., Setou, T., Komatsu, K., 2009. Water mass variability in the western North Pacific detected in a 15-year eddy resolving ocean reanalysis. J. Oceanogr. 65, 737-756. https://doi.org/10.1007/s10872-009-0063-3.
- Miyazawa, Y., Varlamov, S.M., Miyama, T., Guo, X., Hihara, T., Kiyomatsu, K., Kachi, M., Kurihara, Y., Murakami, H., 2017. Assimilation of high-resolution sea surface temperature data into an operational nowcast/forecast system around Japan using a multi-scale three-dimensional variational scheme. Ocean Dyn. 67, 713–728. https://doi.org/10.1007/s10236-017-1056-1.
- Oba, T., Irino, T., 2012. Sea level at the last glacial maximum, constrained by oxygen isotopic curves of planktonic foraminifera in the Japan Sea. J. Quat. Sci. 27, 941–947. https://doi.org/10.1002/jqs.2585.
- Sanganyado, E., Chingono, K.E., Gwenzi, W., Chaukura, N., Liu, W., 2021. Organic pollutants in deep sea: occurrence, fate, and ecological implications. Water Res. 205, 117658. https://doi.org/10.1016/j.watres.2021.117658.
- Schulz-Bull, D.E., Petrick, G., Bruhn, R., Duinker, J.C., 1998. Chlorobiphenyls (PCB) and PAHs in water masses of the northern North Atlantic. Mar. Chem. 61, 101–114. https://doi.org/10.1016/S0304-4203(98)00010-3.
- Sinkkonen, S., Paasivirta, J., 2000. Degradation half-life times of PCDDs, PCDFs and PCBs for environmental fate modeling. Chemosphere 40, 943–949. https://doi.org/ 10.1016/S0045-6535(99)00337-9.
- Sobek, A., Gustafsson, Ö., 2014. Deep water masses and sediments are main compartments for polychlorinated biphenyls in the Arctic Ocean. Environ. Sci. Technol. 48, 6719–6725. https://doi.org/10.1021/es500736q.
- Sobek, A., Gustafsson, Ö., Hajdu, S., Larsson, U., 2004. Particle—water partitioning of PCBs in the photic zone: a 25-month study in the open Baltic Sea. Environ. Sci. Technol. 38, 1375–1382. https://doi.org/10.1021/es034447u.
- Sobek, A., Abel, S., Sanei, H., Bonaglia, S., Li, Z., Horlitz, G., Rudra, A., Oguri, K., Glud, R.N., 2023. Organic matter degradation causes enrichment of organic pollutants in hadal sediments. Nat. Commun. 14, 2012. https://doi.org/10.1038/ s41467-023-37718-z
- Sun, C., Soltwedel, T., Bauerfeind, E., Adelman, D.A., Lohmann, R., 2016. Depth profiles of persistent organic pollutants in the north and tropical Atlantic Ocean. Environ. Sci. Technol. 50, 6172–6179. https://doi.org/10.1021/acs.est.5b05891.
- Takahashi, S., Karri, R., Tanabe, S., 2014. Contamination by persistent organic pollutants and related compounds in deep-sea ecosystems along frontal zones around Japan. In: The Handbook of Environmental Chemistry. Springer, Berlin Heidelberg, Berlin, Heidelberg, https://doi.org/10.1007/698.2013.252.
- Talley, L.D., Tishchenko, P., Luchin, V., Nedashkovskiy, A., Sagalaev, S., Kang, D.-J., Warner, M., Min, D.-H., 2004. Atlas of Japan (East) Sea hydrographic properties in summer, 1999. In: Progress in Oceanography, Physical and Chemical Processes in the Japan/East Sea and Their Influence on Its Ecosystem, 61, pp. 277–348. https:// doi.org/10.1016/j.pocean.2004.06.011.
- Wagner, C.C., Amos, H.M., Thackray, C.P., Zhang, Y., Lundgren, E.W., Forget, G., Friedman, C.L., Selin, N.E., Lohmann, R., Sunderland, E.M., 2019. A global 3-D

- Ocean model for PCBs: benchmark compounds for understanding the impacts of global change on neutral persistent organic pollutants. Glob. Biogeochem. Cycles 33, 460, 481, https://doi.org/10.1009/2019CB006018
- 469-481. https://doi.org/10.1029/2018GB006018.

 Xie, X.-L., Zhou, W.-T., Zhang, K.-K., Yuan, Y., Qiu, E.-M., Shen, Y.-W., Wang, Q., 2019. PCB52 induces hepatotoxicity in male offspring through aggravating loss of clearance capacity and activating the apoptosis: sex-biased effects on rats. Chemosphere 227, 389-400. https://doi.org/10.1016/j.chemosphere.2019.04.077.
- Yanagi, T., 2002. Water, salt, phosphorus and nitrogen budgets of the Japan Sea. J. Oceanogr. 58, 797–804. https://doi.org/10.1023/A:1022815027968.
- Yang, M., Guo, X., Ishizu, M., Miyazawa, Y., 2022. The Kuroshio regulates the air–sea exchange of PCBs in the Northwestern Pacific Ocean. Environ. Sci. Technol. 56, 12307–12314. https://doi.org/10.1021/acs.est.2c03459.
 Yang, M., Guo, X., Zheng, J., Miyazawa, Y., 2024. North-south discrepancy in the
- Yang, M., Guo, X., Zheng, J., Miyazawa, Y., 2024. North-south discrepancy in the contributors to CB153 accumulation in the deep water of the Sea of Japan. Sci. Total Environ. 939, 173599. https://doi.org/10.1016/j.scitotenv.2024.173599.